Expanded View Figures

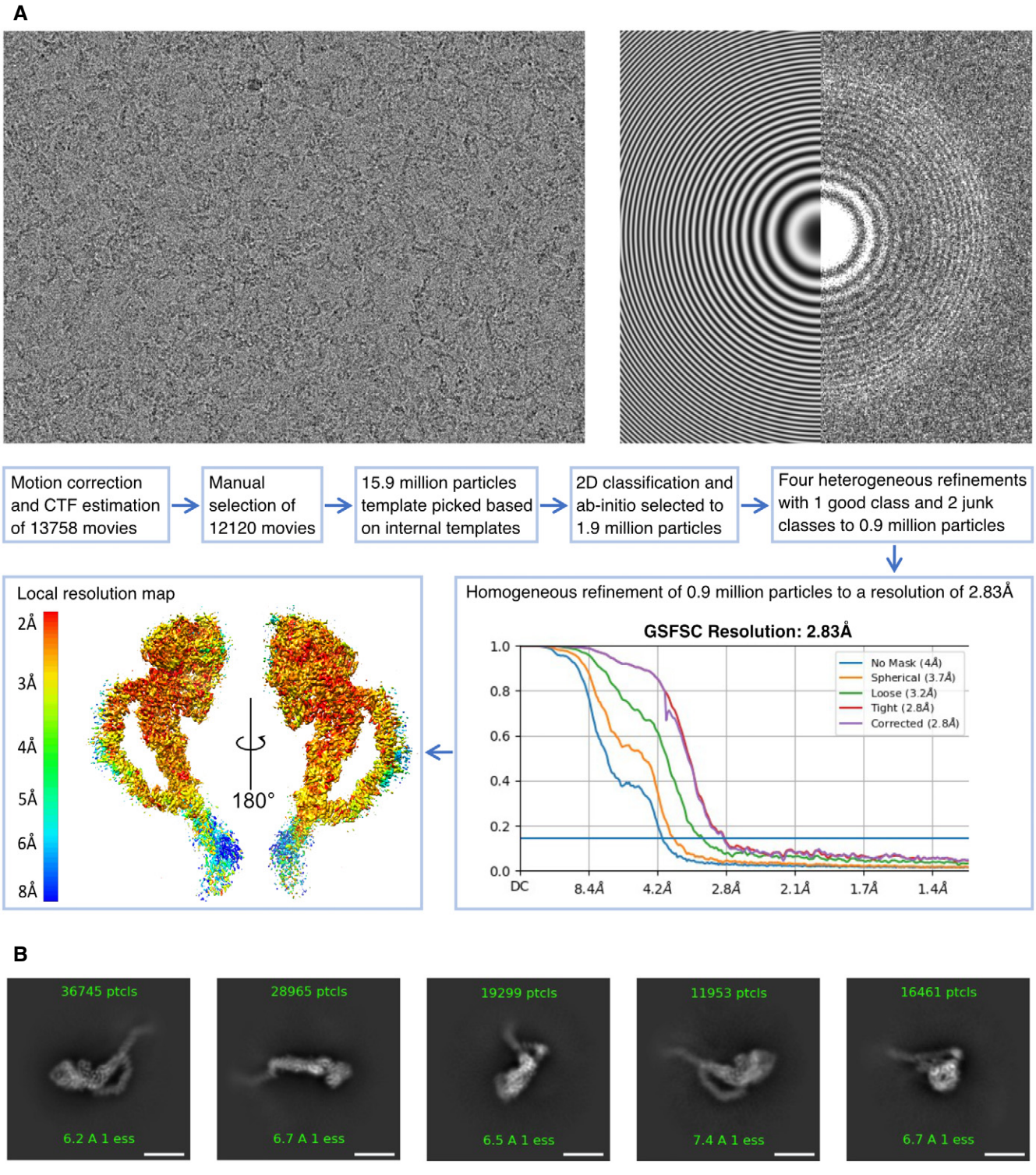

Figure EV1.

© 2021 The Authors

Figure EV1. Road map for obtaining a 2.8 Å resolution cryo-EM map of TcdA.

A Workflow from cryoSPARC processing. Top images show examples of raw micrograph (left) and corresponding contrast transfer function (CTF) fit in Fourier space (right) with theoretical fit shown on the left side and experimental data on the right side. In total, 13,758 movies were processed using patch motion correction and CTF estimation including data curation based on defocus, CTF fit, and motion correction values. The particles were picked using a template based on initial 2D classes from a subset of the data. Good particles were selected using 2D classification and *ab initio* refinements followed by multiple heterogeneous refinement runs and resulted in 0.9 million good particles. A final homogeneous refinement run yielded a map at 2.8 Å resolution based on an FSC threshold of 0.143 (graph bottom right). The resulting map (bottom left) is colored according to local resolution (contoured at 6.7 σ).

B Representative 2D classes of TcdA particles showing side, back, and top views. The region extending from residue 2,383 of the CROPs domain of TcdA is visible in the 2D classes but averaged out in the final 3D map because of high flexibility in this region. Scale bars, 100 Å.

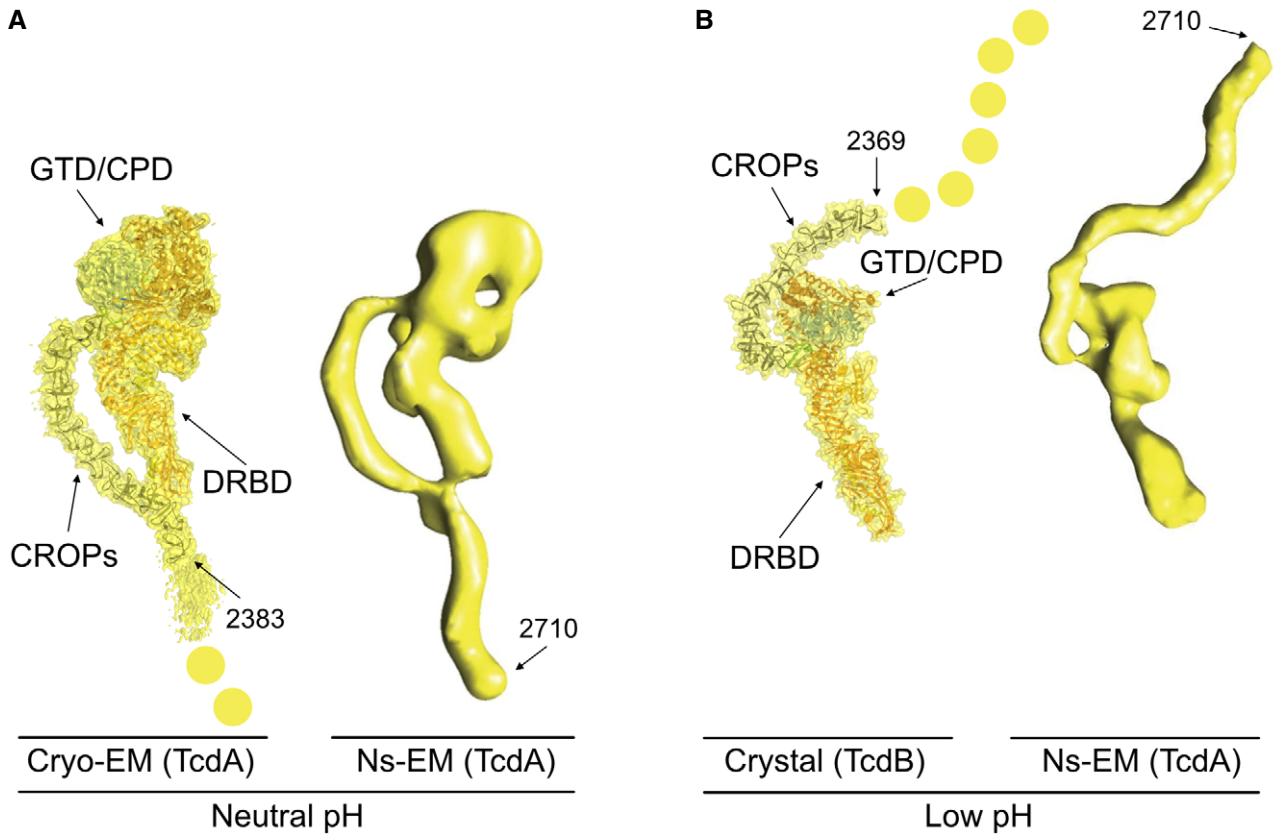

Figure EV2. Comparison of TcdA and TcdB structures.

A Comparison of TcdA and TcdB structures to negative staining EM (Ns-EM) of TcdA. The 2.8 Å cryo-EM map with structure of TcdA modeled into the map next to a negative stain EM map of TcdA at neutral pH (Pruitt *et al*, 2010). Yellow dots extending from the cryo-EM map represent the C-terminal part of the CROPs which is averaged out in the final 3D map.

B Crystal structure of TcdB at pH 5.2 with a reoriented CROPs domain (Chen *et al*, 2019) compared to a negative stain EM map of TcdA at pH 4.5 (Pruitt *et al*, 2010). Yellow dots represent the C-terminal part of the CROPs domain, which is present in TcdA but not in TcdB. Negative stain EM images from Pruitt *et al*, 2010, are used with permission from PNAS.

© 2021 The Authors

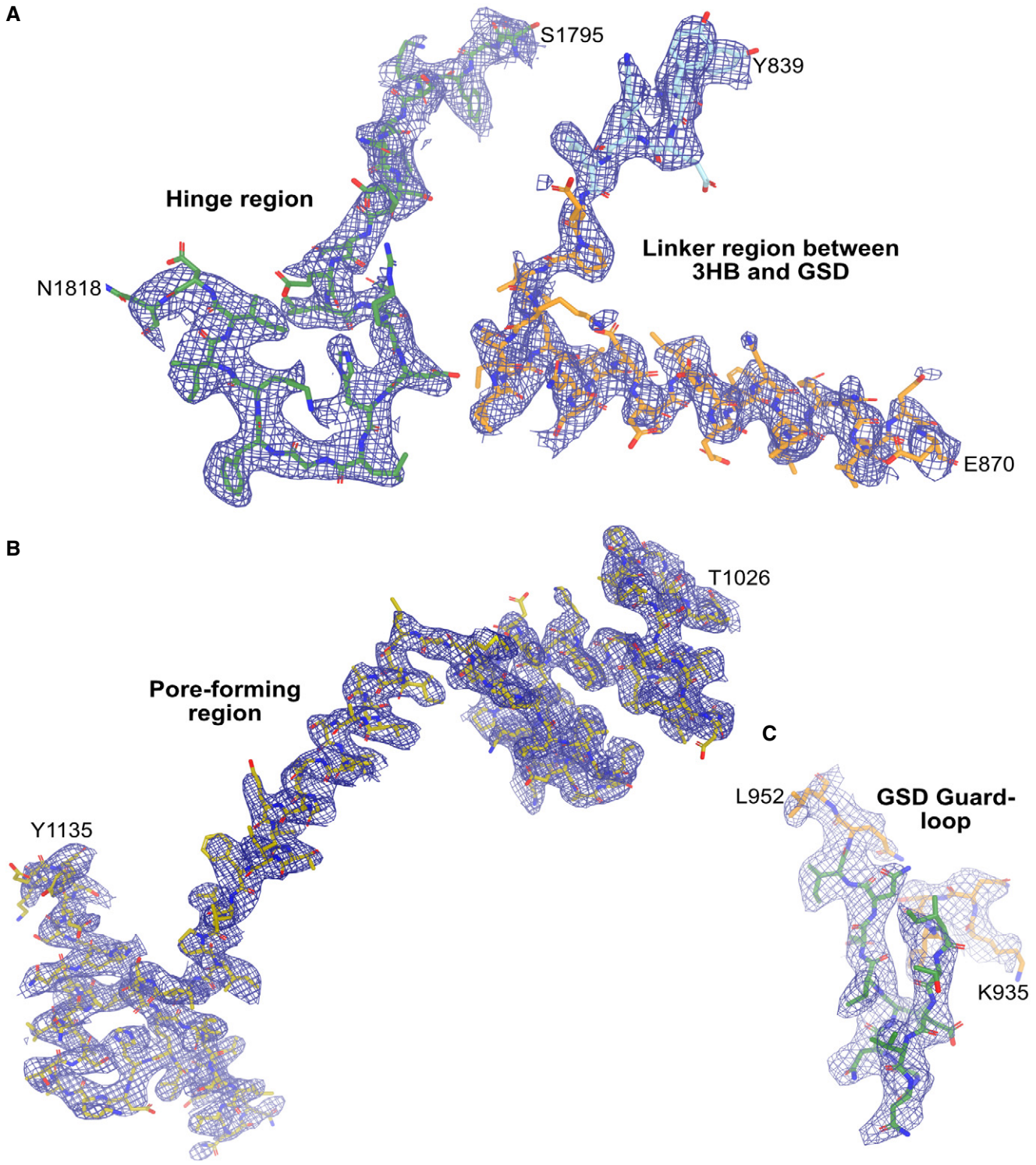

Figure EV3. The 2.8 Å cryo-EM map presented in different regions of the TcdA structure.

A Map of the hinge region (residues 1,795–1,818) as well as the linker region between the 3HB and the GSD (residues 839–870).
B Map of the entire pore-forming region from residues 1,026–1,135.
C Map of the guard loop in GSD from residues 936–952. All maps are contoured at 8 σ.

© 2021 The Authors

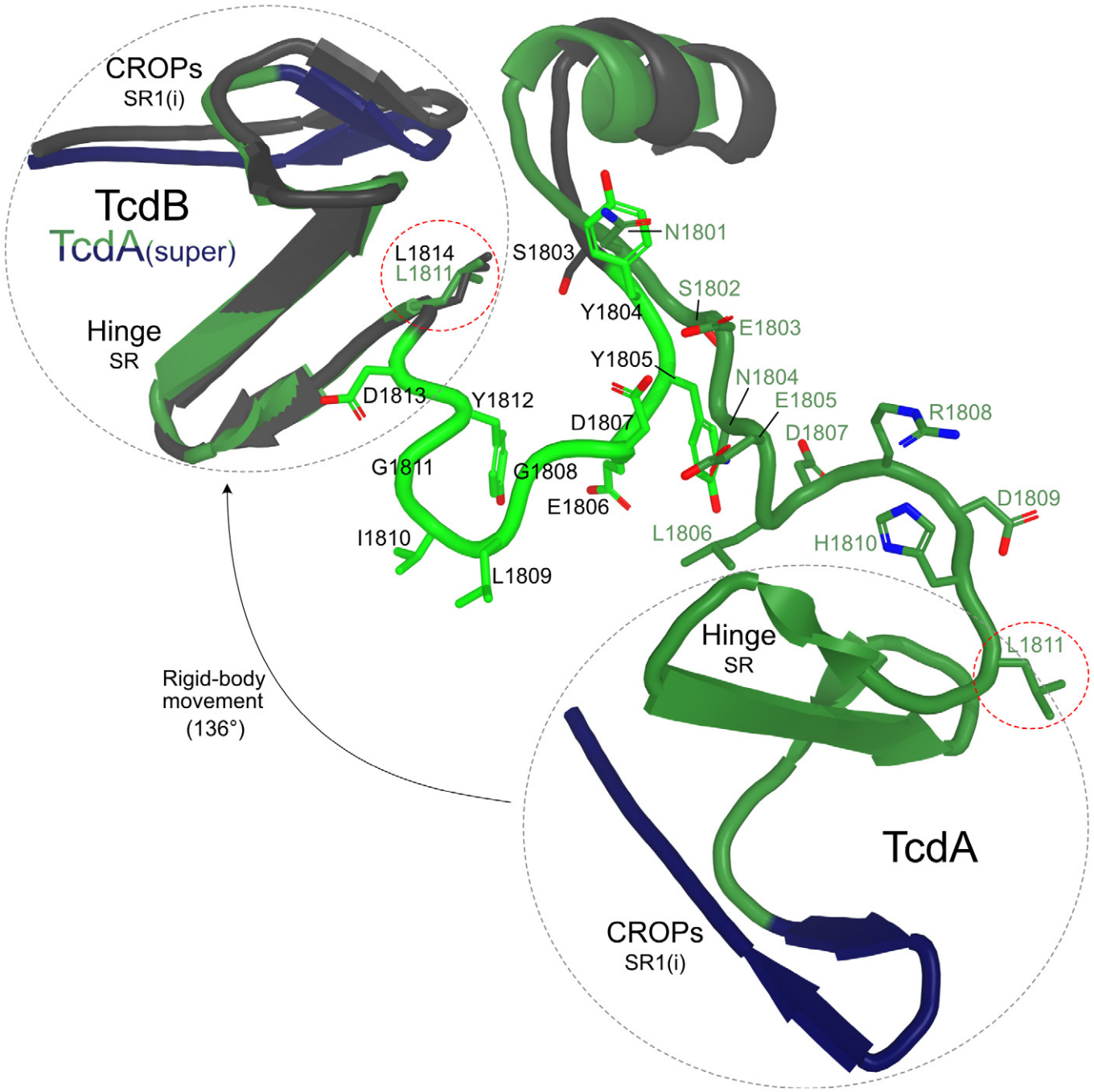

Figure EV4. Movement of the hinge SR and CROPs SR1 during acidification.

Close-up view showing the rigid body movement of the TcdA hinge SR (dark green) and the SR1 of the CROPs domain (dark blue) in a superposition of the TcdA and TcdB CROPs domains. The ~136° rotation of the hinge region and CROPs region relative to the GTD and the CPD is displayed by the superimposed hinge SR and SR1 of the CROPs domain of TcdA on the corresponding regions of TcdB at low pH (dark gray). This rotation is primarily facilitated by changes in the backbone conformations of residues Ser1802 to His1810 of the hinge loop in TcdA (Tyr1805-Asp1813 in TcdB (light green)). The red circle highlights the movement of Leu1811 during acidification, while the gray circle highlights movement of hinge SR and CROPs SR1.

© 2021 The Authors

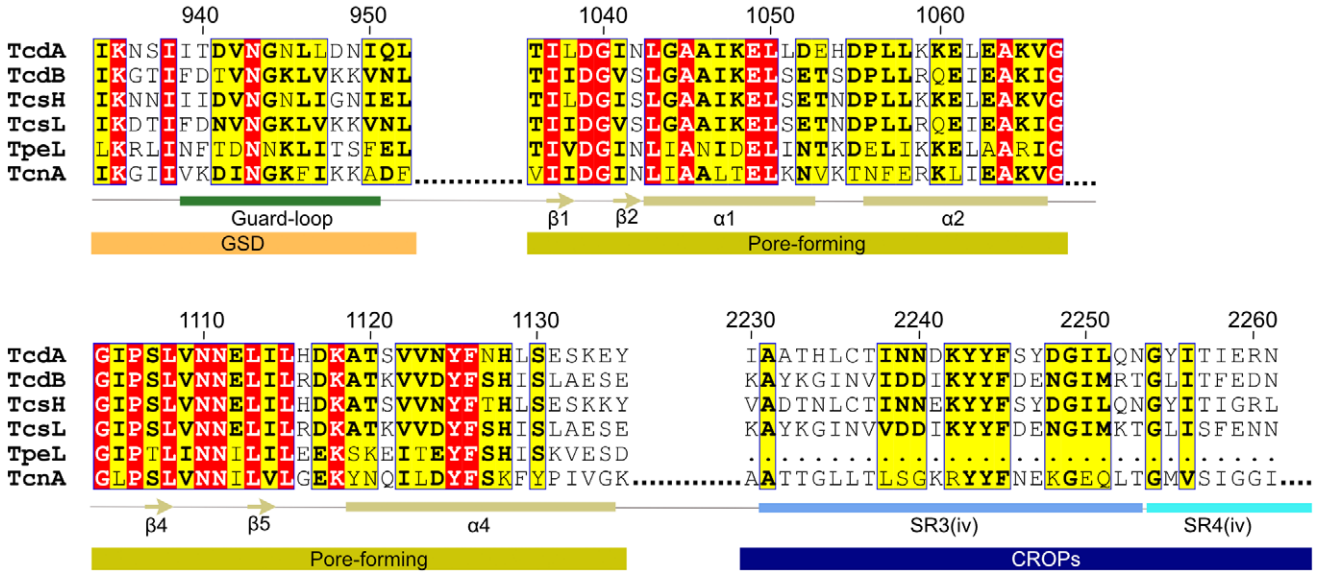

Figure EV5. Alignment of large clostridial cytotoxins.

Amino acid sequence alignment of the guard loop in the GSD, part of the pore-forming region, and SR3 (iv) and SR4 (iv) of the CROPs domain among the large clostridial cytotoxins. TcdA and TcdB originate from *C. difficile* strain R20291, TcsH and TcsL are both from *C. sordellii* strain VPI 9048, TpeL originates from *C. perfringens* strain CP4, and TcnA is from *C. novyi* B strain NCTC 9691.

© 2021 The Authors